25th ABCM International Congress of Mechanical Engineering
October 20-25, 2019, Uberlândia, MG, Brazil

COB-2019-1863
COUPLING FINITE ELEMENTS APPLIED TO HYDRAULIC ANALYSIS IN SATURATED POROUS MEDIA

Murilo Camargo
murilo.camargo@unesp.br
Pedro R. Cleto
pedro.cleto@unesp.br
Eduardo A. Rodrigues
eduardo.alexandre@unesp.br
Heber A. A. Fabbri
heber.fabbri@unesp.br
Osvaldo L. Manzoli
osvaldo.l.manzoli@unesp.br

São Paulo State University - UNESP - Bauru/SP - Av. Eng. Luiz Edmundo Coube, 14-01, CEP: 17033-360

Abstract. *This paper presents a new methodology to couple non-matching Finite Element (FE) meshes used to model fluid flow in saturated porous media. The proposed technique is based on the definition of Coupling Finite Elements (CFEs), which are strategically employed to ensure the continuity of pressure between independent (non-matching) FE meshes. This technique is particularly powerful to handle cases where specific regions of the material need to be discretized with highly refined FE meshes. In addition, the non-matching meshes are coupled without increasing the total number of degrees of freedom of the problem. Two numerical examples (2D problem) with non-matching meshes are analyzed to validate the proposed method. The results obtained for the matching and non-matching meshes are similar, demonstrating the efficiency of the method.*

Keywords: *Darcy's law, non-matching meshes, coupling finite elements, porous media*

1. INTRODUCTION

Numerical modeling and simulation of fluid flow in porous media has received increasing attention mainly due to the computational development. The finite element method (FEM) is one of the techniques widely used to solve this kind of problem and its accuracy is directly associated with the mesh discretization. However, refined meshes require more computational effort when compared to coarse meshes. A possible solution to overcome that issue is to subdivide the domain into fully independent subdomains with different degrees of refinement and use coupling techniques to connect the non-matching meshes. This strategy has been applied in adaptive mesh refinement (Wu *et al.* (2009), Lo *et al.* (2010) and Lim *et al.* (2012)), multiphysical analysis (Dureisseix and Bavestrello (2006), Hüeber and Wohlmuth (2009) and Bazilevs *et al.* (2012)) and multiscale problems (Unger and Eckardt (2011), Lloberas-Valls *et al.* (2012) and Thirunavukkarasu and Guddati (2012)).

In multiphysical problems, de Boer *et al.* (2007) compare six distinct methods to deal with the transfer of information between non-matching meshes, which are based on: nearest neighbour interpolation (Thévenaz *et al.*, 2000); an orthogonally designed point of another mesh (Farhat *et al.* (1998), Cebral and Lohner (1997) and Loehner *et al.* (1998)); splines interpolation (Thévenaz *et al.*, 2000); radial basis functions (Smith *et al.*, 2000); Lagrange multipliers (Ransom, 2002) and optimal way, also named by Mortar method (Baaijens, 2001).

In the context of mechanical problems, Bitencourt Jr *et al.* (2015) proposed an approach to coupling non-matching meshes, based on the use of coupling finite elements (CFE). The applicability of the technique was illustrated for different $2D$ and $3D$ examples. The authors demonstrated that the CFEs can ensure continuity of the displacement field, without increasing the number of degrees of freedom of the problem. Rodrigues *et al.* (2018) used the same CFEs for the adaptive concurrent multiscale modeling of concrete.

The CFE technique was successfully used by Vafajou *et al.* (2018) to study the behavior of the fluid flow in a naturally fractured porous medium. The authors inserted the discontinuities in the mesh using the coupling elements and compared the performance of this technique against other numerical methods.

This paper presents the application of CFEs to couple non-matching meshes to model the behavior of fluid flow in

domains with different permeabilities. The numerical 2D hydraulic examples compare the pressure fields obtained from matching and non-matching meshes.

2. GOVERNING EQUATIONS FOR HYDRAULIC PROBLEMS

Considering an isotropic medium, the fluid flow given by Darcy's Law can be written by:

$$\mathbf{q} = -\frac{\kappa}{\mu}(\boldsymbol{\nabla} p - \rho_f \mathbf{g}) \tag{1}$$

where, $\mathbf{q}$ is the flux vector, κ represents the intrinsic permeability of the porous medium, μ is the fluid viscosity, $\boldsymbol{\nabla} p$ is the gradient of pressure, ρ_f is the specific mass of the fluid and $\mathbf{g}$ is the gravity acceleration.

The fluid mass conservation equation for the permanent regime can be written as:

$$\boldsymbol{\nabla} \cdot \mathbf{q} = 0 \tag{2}$$

The boundary conditions of the hydraulic problem are given by $p = \bar{p}$ on Γ_p and $\mathbf{q} \cdot \mathbf{n} = \bar{q}$ on Γ_q, where $\bar{p}$ and $\bar{q}$ are the pressure and flow prescribed on the boundaries Γ_p e Γ_q, respectively.

3. COUPLING FINITE ELEMENTS (CFEs)

Figure 1 illustrates the technique proposed by Bitencourt Jr *et al.* (2015) where the domain (Ω) is subdivided into two other subdomains, Ω^1 and Ω^2, discretized with non-matching meshes. As a consequence, the interface $\Gamma_{12} = \Gamma_1 \cap \Gamma_2$ of these subdomains is a non-matching interface containing loose nodes, represented in blue in Fig. 1.

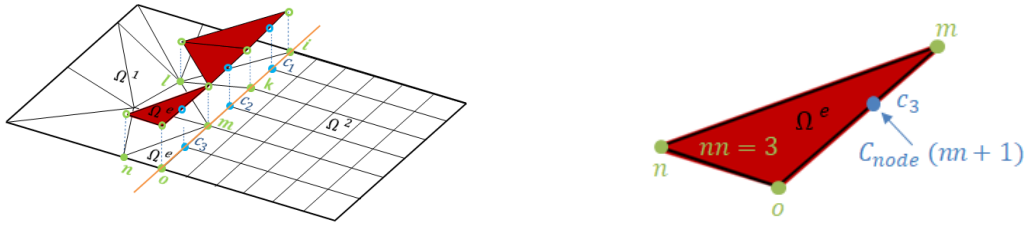

a) b)

Figure 1: Coupling technique for non-matching FE meshes. a) Coupling procedure for 2D problem with two non-matching meshes. b) Triangular coupling FE. (adapted from Bitencourt Jr *et al.* (2015)).

This coupling between the meshes is based on the insertion of Coupling Finite Elements (CFEs), shown in red in Fig. 1a. The CFEs are derived from standard isoparametric finite element by adding one extra node, called coupling node (C_{node}). Since these elements share nodes of both meshes, no additional degrees of freedom are introduced to the problem. Another advantage is that the technique can be easily incorporated into a conventional FE code, since no special formulation or integration scheme are required.

3.1 CFEs Formulation

The pressure field at any material point $\mathbf{X}$ inside a finite element can be approximated in terms of its nodal pressures by:

$$\mathbf{P(X)} = \sum_{i}^{nn} N_i(\mathbf{X}) p_i \tag{3}$$

where nn is the number of nodes of the element, $N_i(\mathbf{X})(i = 1, nn)$ are the standard shape functions and p_i are the nodal pressures.

In order to establish a connection between the non-matching meshes, the difference between the pressure at the coupling node, C_{node} , and its corresponding material point ($\mathbf{X}_c$) is calculated using the standard shape functions $N_i(\mathbf{X}_c)$, as follows:

$$[\![\mathbf{P}]\!] = \mathbf{P}_{nn+1} - \mathbf{P}(\mathbf{X}_c) = \mathbf{P}_{nn+1} - \sum_{i}^{nn} N_i(\mathbf{X}_c) p_i = \mathbf{B}_e \mathbf{P}_e \tag{4}$$

where $[\![\mathbf{P}]\!]$ is the relative pressure and $\mathbf{B}_e$ and $\mathbf{P}_e$ are given by:

$$\mathbf{B}_e = [-\mathbf{N}_1(\mathbf{X}_c) \quad -\mathbf{N}_2(\mathbf{X}_c)... \quad -\mathbf{N}_{nn}(\mathbf{X}_c) \quad \mathbf{1}] \tag{5}$$

$$\mathbf{P}_e = [p_1 \quad p_2... \quad p_{nn} \quad p_{nn+1}]^T \tag{6}$$

Exploring the correspondence between mechanical and hydraulic problems (Segura and Carol (2004) and Vafajou *et al.* (2018)) the internal virtual work δW^{int} for the CFE is given by:

$$\delta W^{int} = \delta[\![\mathbf{P}]\!]\mathbf{q}([\![\mathbf{P}]\!]) \tag{7}$$

where $\mathbf{q}([\![\mathbf{P}]\!])$ is the flux associated with the relative pressure $[\![\mathbf{P}]\!]$ and $\delta[\![\mathbf{P}]\!]$ is an arbitrary virtual relative pressure. Using the same approximation for the relative pressure and the virtual relative pressure given by Eq. 5, the internal flow vector $\mathbf{q}_e^{int}$ and the corresponding permeability matrix $\mathbf{K}_e$ can be obtained by:

$$\mathbf{q}_e^{int} = \mathbf{B}_e^T \mathbf{q}([\![\mathbf{P}]\!]) \tag{8}$$

$$\mathbf{K}_e = \frac{\partial \mathbf{q}_e^{int}}{\partial \mathbf{P}_e} = \mathbf{B}_e^T \mathbf{C} \mathbf{B}_e \tag{9}$$

where, $\mathbf{C}$ is a matrix of constants assuming high values that play the rule of penalty factors enforcing a null pressure drop ($[\![\mathbf{P}]\!] = 0$), allowing the coupling of the non-matching meshes.

4. NUMERICAL EXAMPLES

The main purpose of the numerical examples is verify the ability of the CFEs to solve hydraulic problems. Therefore, to simplify the model, gravitational effects are disregarded and all the domains are completely saturated by only one fluid. The problems are divided in two cases: (i) insertion and (ii) application cases.

4.1 Insertion case

Subdomains with the same permeability

The first example considers a stationary fluid flow in a 1.2×1.2 m 2-dimensional fully saturated porous medium. The domain is composed of two subdomains, Ω^1 and Ω^2, where Ω^2 is surrounded by Ω^1 (Fig. 2). In order to test the CFE method, different discretizations are adopted for Ω^1, i.e. a refined (Mesh A) and a coarse (Mesh B) meshes (Fig. 2a,b, respectively), while Ω^2 remains with the same discretization. Thus, the total domain presents a matching mesh (Mesh A) and a non-matching mesh (Mesh B). Therefore, in the Mesh B (coarse), Ω^1 is coupled to the Ω^2 via CFEs (Fig. 2b).

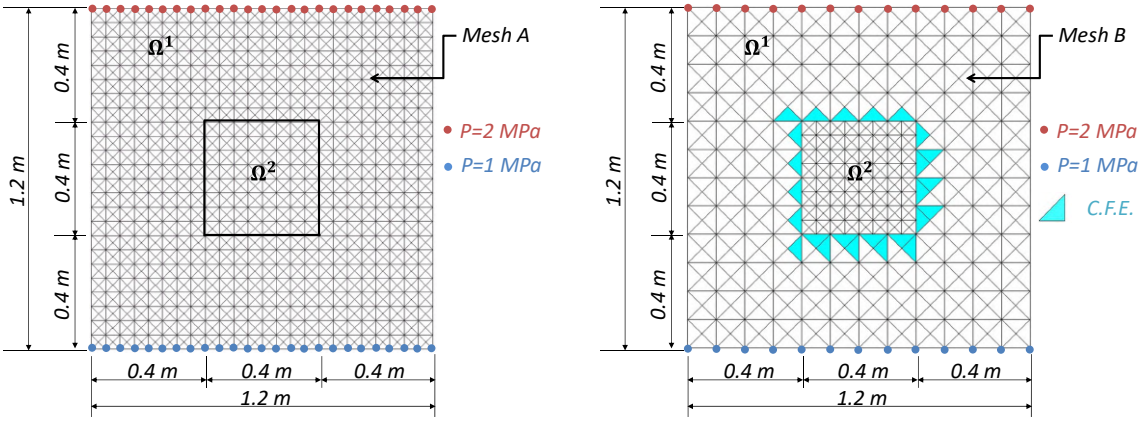

(a) (b)

Figure 2: Sample with square geometry discretized by: a) matching triangular FEs. b) non-matching triangular FEs with two different scales of refinement.

The coupling between the meshes is verified imposing a pressure gradient ($\Delta p = 1.0$ MPa) in the whole domain. In this case, Ω^1 and Ω^2 have the same permeability, i.e. $k_{\Omega^1} = k_{\Omega^2} = 1.0 \times 10^{-15}$ m^2. Figures 3a and 3b shows the

pressure field in both meshes. Figure 3c compares the pressure along different heights ($y_1 = 0.3m, y_2 = 0.4m, y_3 = 0.6m, y_4 = 0.8m, y_5 = 0.9m$), where M represents the matching mesh, while NM represents the non-matching meshes. The good agreement between the responses obtained using matching and non-matching meshes shows that CFEs were able to couple the non-matching meshes.

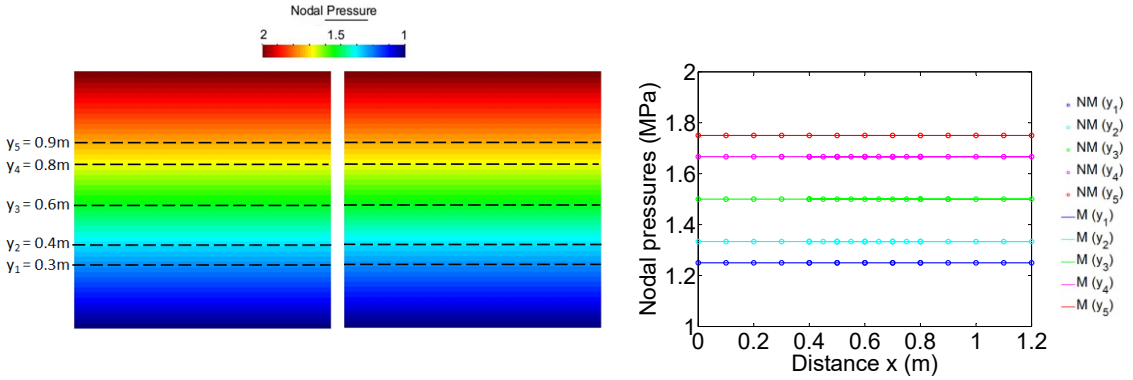

(a) (b) (c)

Figure 3: First example. Pressure field of the (a) matching and (b) non-matching meshes and (c) convergence analysis between the meshes.

Subdomains with different permeability

In the second case, the permeability of Ω^2 was replaced by $k_{\Omega^2} = 1.0 \times 10^{-14}\text{m}^2$. Figures 4a and 4b show the pressure field for both meshes. As expected, the higher permeability associated to Ω^2 disturbs the pressure field, since the more permeable region induces a preferential pathway to the fluid flow.

Figure 4c presents a comparison between the results from the distinct meshes along different heights ($y_1 = 0.3m, y_2 = 0.4m, y_3 = 0.6m, y_4 = 0.8m, y_5 = 0.9m$). In this case, a good agreement is also obtained, indicating an efficient coupling between non-matching meshes.

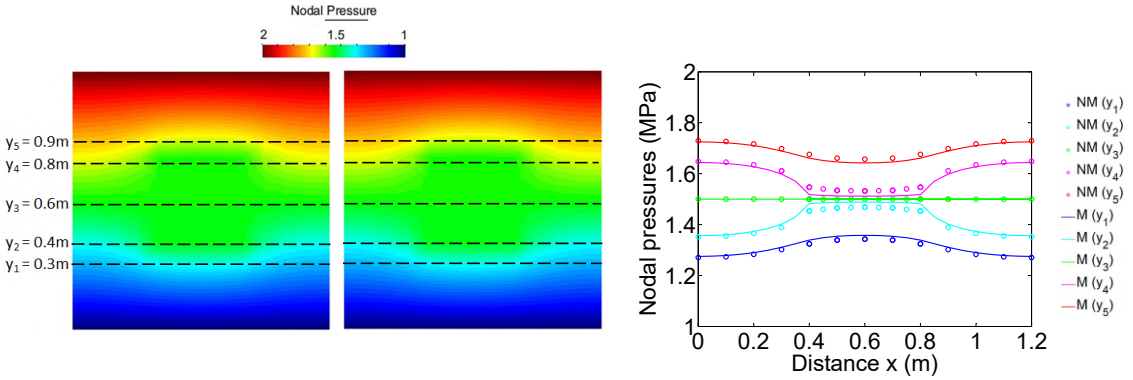

(a) (b) (c)

Figure 4: Second example. Pressure field of the (a) matching and (b) non-matching meshes and (c) convergence analysis between the meshes.

For this second example, the equivalent permeability of each mesh (i.e. matching and non-matching meshes) was calculated according to the total flow rate leaving from only one boundary with prescribed pressure. The following expression gives the equivalent permeability:

$$K_{eq} = -\sum_{i=1}^{nnp} Q_i \frac{\mu L}{A \Delta p} \tag{10}$$

where Q_i is the flow rate in the node i, nnp is the number of nodes in the boundary, Δp is the pressure difference, L is the distance between the boundaries with prescribed pressures and A is the area of the boundary (for a unitary thickness, A = L). Table 1 compares these permeabilities, where is possible verify similar results. Note that, considering that the matching mesh provides a more accurate result, the relative error (difference) is less than 0.4%.

Table 1: Values of the equivalent permeabilities K_{eq}.

Equivalent Permeability - K_{eq}	
	K_{eq} (m^2)
Matching Meshes	1.215250376E-15
Non-Matching Meshes	1.219482775E-15
Relative Error	0.352%

4.2 Application case: geologic fault

The second numerical case considers a fully saturated reservoir sectioned by a geologic fault and isolated by two other regions (Overburden and Underburden), where each adopted intrinsic permeability is presented in Table 2. Two wells (injection and production) are positioned within the reservoir on opposite sides to the fault as show in Fig. 5. The injection well operates at a constant pressure equal to $4MPa$, while the production well operates at a constant pressure equal to $-4MPa$ (Fig. 5).

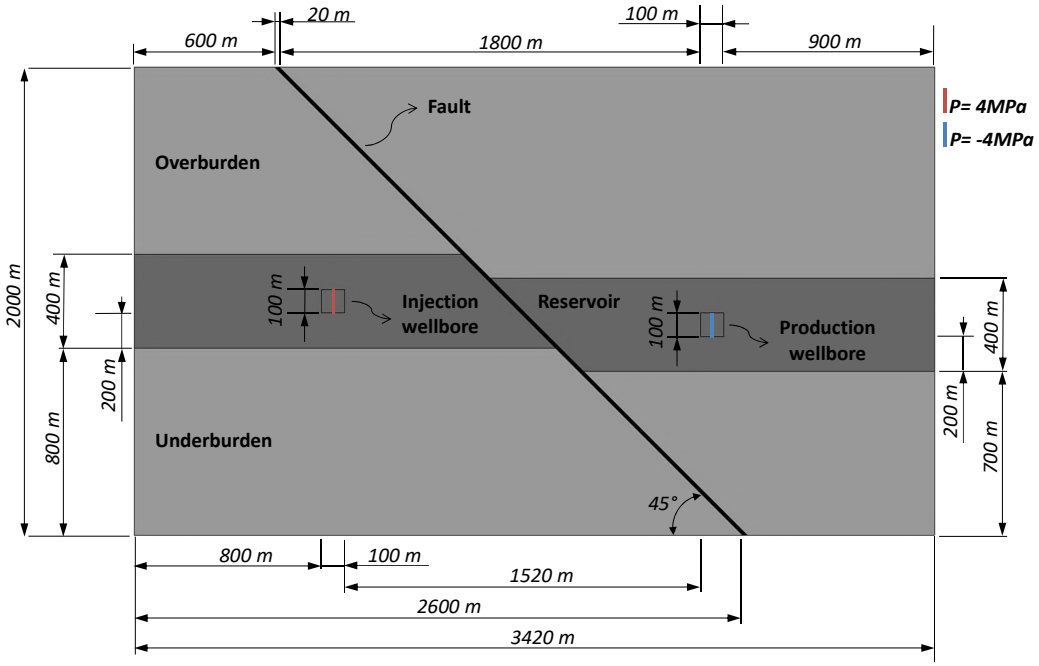

Figure 5: Schematic representation for the second case.

Table 2: Values of the permeabilities of materials (k).

	Reservoir	Fault	Overburden and Underburden
$k(m^2)$	1.0×10^{-12}	1.0×10^{-14}	1.0×10^{-22}

In order to verify the efficiency of the CFE technique, a comparison between matching and non-matching meshes in terms of pressure field was performed. Figure 6 illustrates the matching mesh configuration obtained for the entire domain, Ω^M domain. Figure 7 shows the steps for the construction of the non-matching mesh, since the domain Ω^{NM} corresponds to the union of the independent subdomains Ω^1, Ω^2, Ω^3 and Ω^4. The number of elements used for construction of the matching mesh was 61,124, while for non-matching mesh was 46,402 elements. This reduction in the number of elements represents a decrease in the computational effort, once the degrees of freedom of the problem are also reduced by using a more optimized mesh.

Figures 8a and 8b show the pressure field for matching (M) and non-matching mesh (NM), respectively. A good similarity between the pressure fields can be observed. Figures 9a, 9b and 9c represent the values of nodal pressures along sections $S1$, $S2$ and $S3$, respectively. Section $S1$ is located at a height of $950m$ and is mostly contained within the reservoir, since, in its central part, the section crosses the fault. Sections $S2$ and $S3$ are located at a distance of $850m$ and $2470m$, respectively, and cross the four regions (Underburden, Reservoir, Overburden and Fault). It is noted that all three sections chosen have, at least, an interface region between the meshes, which allows evaluating the critical points of the technique of CFEs. Figures 9b and 9c for example, highlight part of the curve that represents the transition region

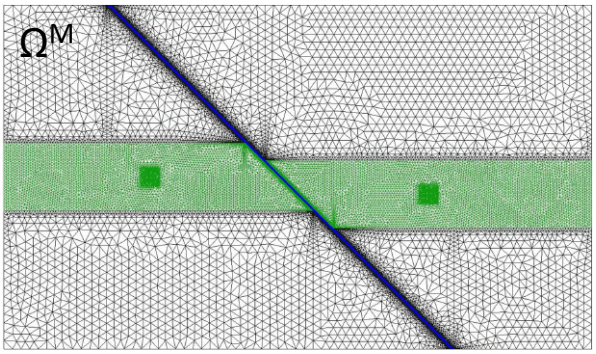

(a)

Figure 6: Geometry discretized by matching triangular FEs.

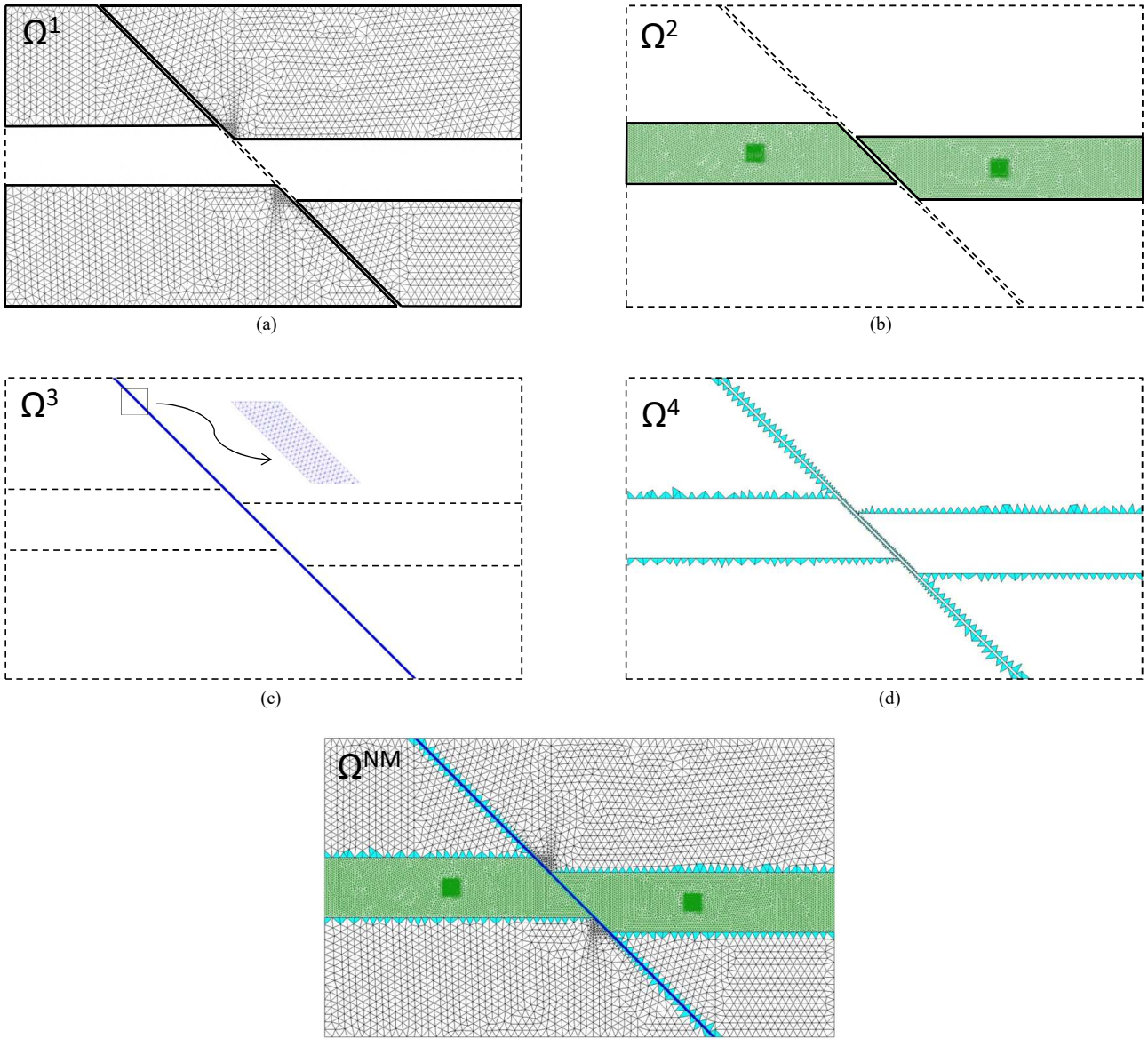

(a) (b) (c) (d) (e)

Figure 7: Non-matching mesh construction. (a) Underburden and Overburden meshes. (b) Reservoir mesh. (c) Fault mesh. (d) Creation of CFEs to couple all subdomains. (e) Geometry discretized by the CFEs technique.

between Underburden/Overburden and fault. Similarly the matching mesh, the non-matching mesh can also characterize the continuity between the regions.

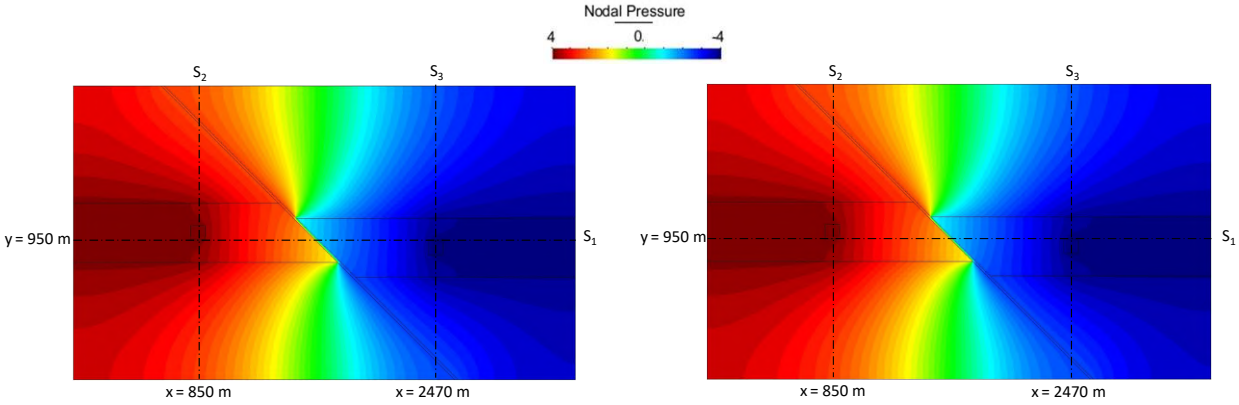

Figure 8: Second example. Pressure field of the (a) matching and (b) non-matching meshes.

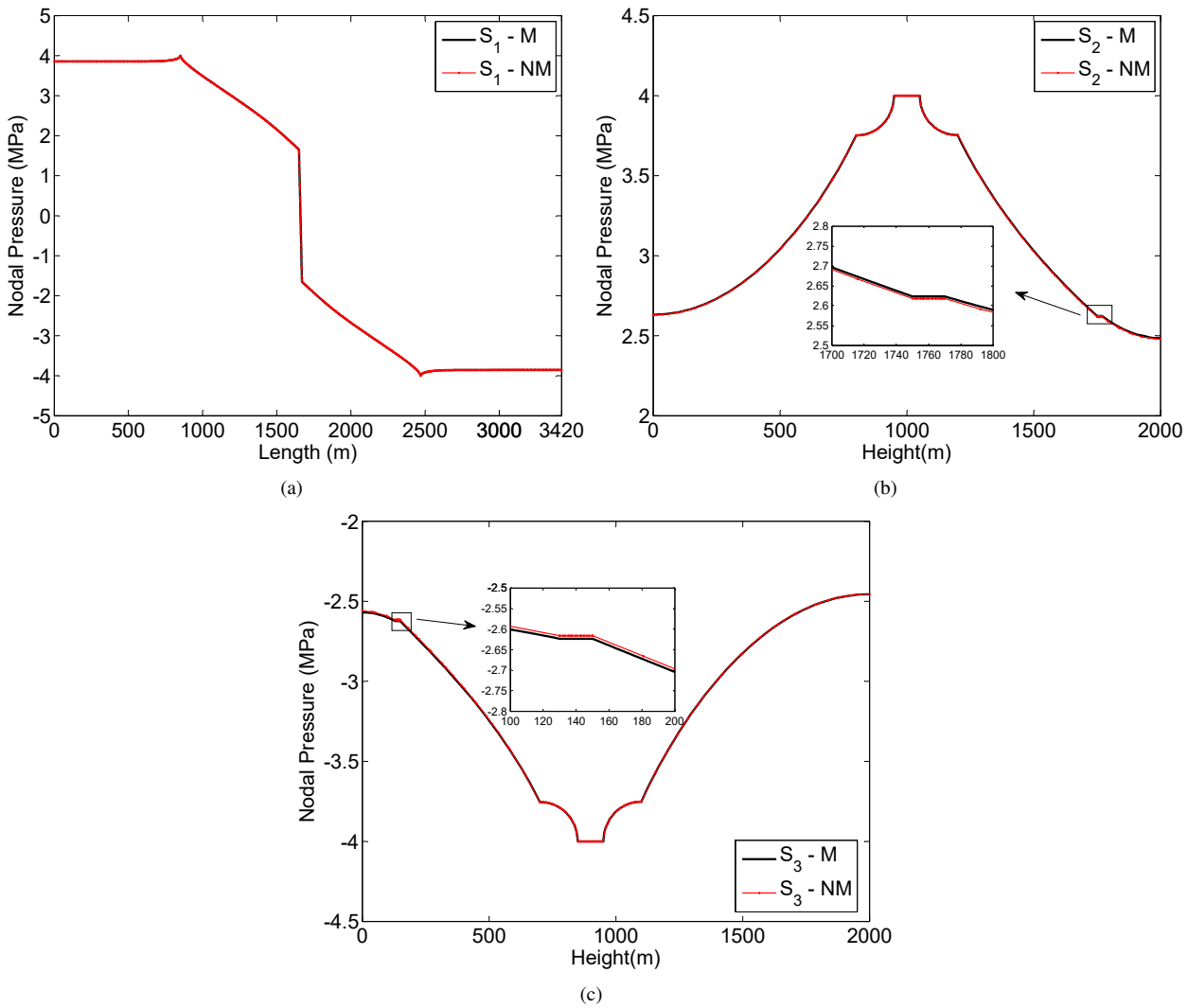

Figure 9: Convergence analysis of nodal pressures along section: (a) $S1$, (b) $S2$ and (c) $S3$ between the matching mesh (M) and non-matching mesh (NM).

5. CONCLUDING REMARKS

The coupling finite element technique proposed by Bitencourt Jr *et al.* (2015) for mechanical problems was properly adapted to couple non-matching meshes applied to simulate hydraulic problems, which showed able to model the behavior of fluid flow in saturated porous media represented by independent FE meshes. The bidimensional examples performed in this work demonstrated the ability of this new technique to couple non-matching meshes, ensuring the correct continuity of pressure field between domains with different mesh discretizations. Moreover, CFEs allows reducing the computational cost, once the degrees of freedom of the problem are reduced by using more optimized meshes.

6. ACKNOWLEDGEMENTS

The authors wish to acknowledge the financial support of the Coordenação de Aperfeiçoamento de Pessoal de Nível Superior – Brasil (CAPES) – Finance Code 001, the National Council for Scientific and Technological Development (CNPq) and Petrobras (under agreement No. 2018/00205-5).

7. REFERENCES

Baaijens, F.P., 2001. "A fictitious domain/mortar element method for fluid–structure interaction". *International Journal for Numerical Methods in Fluids*, Vol. 35, No. 7, pp. 743–761.

Bazilevs, Y., Hsu, M.C. and Scott, M., 2012. "Isogeometric fluid–structure interaction analysis with emphasis on non-matching discretizations, and with application to wind turbines". *Computer Methods in Applied Mechanics and Engineering*, Vol. 249, pp. 28–41.

Bitencourt Jr, L.A., Manzoli, O.L., Prazeres, P.G., Rodrigues, E.A. and Bittencourt, T.N., 2015. "A coupling technique for non-matching finite element meshes". *Computer Methods in Applied Mechanics and Engineering*, Vol. 290, pp. 19–44.

Cebral, J.R. and Lohner, R., 1997. "Conservative load projection and tracking for fluid-structure problems". *AIAA journal*, Vol. 35, No. 4, pp. 687–692.

de Boer, A., Van Zuijlen, A. and Bijl, H., 2007. "Review of coupling methods for non-matching meshes". *Computer methods in applied mechanics and engineering*, Vol. 196, No. 8, pp. 1515–1525.

Dureisseix, D. and Bavestrello, H., 2006. "Information transfer between incompatible finite element meshes: application to coupled thermo-viscoelasticity". *Computer Methods in Applied Mechanics and Engineering*, Vol. 195, No. 44-47, pp. 6523–6541.

Farhat, C., Lesoinne, M. and Le Tallec, P., 1998. "Load and motion transfer algorithms for fluid/structure interaction problems with non-matching discrete interfaces: Momentum and energy conservation, optimal discretization and application to aeroelasticity". *Computer methods in applied mechanics and engineering*, Vol. 157, No. 1-2, pp. 95–114.

Hüeber, S. and Wohlmuth, B., 2009. "Thermo-mechanical contact problems on non-matching meshes". *Computer Methods in Applied Mechanics and Engineering*, Vol. 198, No. 15-16, pp. 1338–1350.

Lim, J.H., Sohn, D. and Im, S., 2012. "Variable-node element families for mesh connection and adaptive mesh computation". *Structural Engineering and Mechanics*, Vol. 43, No. 3, pp. 349–370.

Lloberas-Valls, O., Rixen, D., Simone, A. and Sluys, L., 2012. "On micro-to-macro connections in domain decomposition multiscale methods". *Computer Methods in Applied Mechanics and Engineering*, Vol. 225, pp. 177–196.

Lo, S., Wu, D. and Sze, K., 2010. "Adaptive meshing and analysis using transitional quadrilateral and hexahedral elements". *Finite Elements in Analysis and Design*, Vol. 46, No. 1-2, pp. 2–16.

Loehner, R., Yang, C., Cerbal, J., Baum, J., Luo, H., Pelessone, D. and Charman, C., 1998. "Fluid-structure-thermal interaction using a loose coupling algorithm and adaptive unstructured grids". In *29th AIAA, Fluid Dynamics Conference*. p. 2419.

Ransom, J., 2002. "A multifunctional interface method for coupling finite element and finite difference methods: Two-dimensional scalar-field problems". In *43rd AIAA/ASME/ASCE/AHS/ASC Structures, Structural Dynamics, and Materials Conference*. p. 1573.

Rodrigues, E.A., Manzoli, O.L., Bitencourt Jr, L.A., Bittencourt, T.N. and Sánchez, M., 2018. "An adaptive concurrent multiscale model for concrete based on coupling finite elements". *Computer Methods in Applied Mechanics and Engineering*, Vol. 328, pp. 26–46.

Segura, J. and Carol, I., 2004. "On zero-thickness interface elements for diffusion problems". *International journal for numerical and analytical methods in geomechanics*, Vol. 28, No. 9, pp. 947–962.

Smith, M.J., Hodges, D.H. and S. Cesnik, C.E., 2000. "Evaluation of computational algorithms suitable for fluid-structure interactions". *Journal of Aircraft*, Vol. 37, No. 2, pp. 282–294.

Thévenaz, P., Blu, T. and Unser, M., 2000. "Interpolation revisited [medical images application]". *IEEE Transactions on medical imaging*, Vol. 19, No. 7, pp. 739–758.

Thirunavukkarasu, S. and Guddati, M.N., 2012. "A domain decomposition method for concurrent coupling of multiscale models". *International Journal for Numerical Methods in Engineering*, Vol. 92, No. 11, pp. 918–939.

Unger, J.F. and Eckardt, S., 2011. "Multiscale modeling of concrete". *Archives of Computational Methods in Engineering*, Vol. 18, No. 3, p. 341.

Vafajou, B., Dias-da Costa, D., Bitencourt, L. and Manzoli, O., 2018. "Coupling finite elements for modelling fluid flow in fractured porous media".

Wu, D., Sze, K.Y. and Lo, S.H., 2009. "Two-and three-dimensional transition element families for adaptive refinement analysis of elasticity problems". *International journal for numerical methods in engineering*, Vol. 78, No. 5, pp. 587–630.